

Supplement of Atmos. Chem. Phys., 15, 9327–9343, 2015
<http://www.atmos-chem-phys.net/15/9327/2015/>
doi:10.5194/acp-15-9327-2015-supplement
© Author(s) 2015. CC Attribution 3.0 License.



Supplement of

The influences of mass loading and rapid dilution of secondary organic aerosol on particle volatility

K. R. Kolesar et al.

Correspondence to: C. D. Cappa (cdcappa@ucdavis.edu)

The copyright of individual parts of the supplement might differ from the CC-BY 3.0 licence.

1 The Supplemental Information provides details on the measurement, analysis, and
2 interpretation of the evaporation of α -pinene + O₃ SOA in a thermodenuder (TD). This includes
3 discussion of (i) the experimental conditions and set-up (ii) specifications of the TD design (iii)
4 characterization of the temperature profile inside the TD (iv) inputs for the kinetic model of
5 evaporation (v) results from fitting Eq. 3 in the main text to all variable C_{OA} experiments and (vi)
6 the best-fit model parameters for the dimer only model.

7 8 **Experimental Set-up**

9 A schematic of the experimental set-up for the experiments outlined in the Main Text is
10 shown in Figure S1. The α -pinene is continuously injected into a stream of filtered house air with
11 a syringe pump (Model NE-1000, New Era Pump Systems Inc). The diluter is only used for the
12 experiments in which the SOA was initially formed at high C_{OA} and then diluted to low C_{OA}.

13 14 **Thermodenuder Characterization**

15 The TD used here is based on the design of Huffman et al. (2008) with several modifications,
16 and a schematic is shown in Figure S2. The active heating section of the TD was comprised of a
17 71 cm long heated section of 2.54 cm outer diameter (OD) (2.21 cm inner diameter, ID) stainless
18 steel tubing. The active heating section was attached to a circular connector that attaches directly
19 to a charcoal denuder. Particles in the charcoal denuder passed through a wire mesh tube (1.9 cm
20 ID) that was 48 cm in length that was surrounded by activated carbon charcoal (Sigma-Aldrich,
21 mesh 4-8) that was encased in an 8.9 cm diameter aluminum housing. Organic vapors were
22 stripped from the gas phase as the airstream passed through the denuder. The mesh tube is
23 attached on one end to a 1.9 cm OD (1.6 cm ID) stainless steel tubing extension that is connected
24 to the actively heated section and that extends into the denuded section by 3.8 cm.

25 As in the Huffman et al. (2008) design, heating is induced by woven mesh heating tape
26 (Electrofilm Manufacturing Co) that is wrapped along the length of the stainless steel tube.
27 However, instead of insulating with a ½-inch layer of fiberglass insulation, the heating tape has
28 been wrapped in aluminum foil. This allows for faster cool down times and faster temperature
29 stepping. The temperature is measured by a thermocouple that is in direct contact with the
30 outside of the heated tube and located at the midpoint of the active heating section, and is
31 controlled by a PID temperature controller (Omega).

1 As the airflow passes from the active heating stage to the denuding stage re-condensation is
2 possible. In order to reduce the occurrence of re-condensation or nucleation, the distance
3 between the active heating zone and the charcoal is kept as short as possible (~4.8 cm). For
4 comparison, this transfer length is approximately a quarter the transfer length in the TD of
5 Huffman et al. (2008). By reducing the transfer length and by maintaining greater thermal
6 contact between the active heating section and the transfer section (compared to Huffman et al.)
7 the amount of re-condensation is lessened since the gas-phase compounds that had evaporated
8 have greater opportunity to adsorb to the activated carbon before cooling occurs.

10 **Temperature Characterization**

11 The longitudinal temperature profile along the centerline of the TD has been characterized.
12 The longitudinal temperature profile is described with respect to (i) the set-point temperature at a
13 constant flow rate and (ii) the sample flow rate at a given temperature. The longitudinal
14 temperature profile of the TD (Figure S3) has three distinct regions: a warming region, a fully
15 heated region where the temperature is approximately constant and a cooling region. The cooling
16 region extends beyond the length of the active heating region into the denuding stage, which is
17 indicated by a thick vertical black line in Figure S3.

18 The warming region is the distance over which the airstream is increasing in temperature and
19 extends from the inlet to the beginning of the operationally defined heated region. The heated
20 region is defined as the region where the temperature varies from the set point temperature by
21 less than 10 percent. The cooling region is the distance over which the airstream decreases in
22 temperature and it extends from the end of the heated region to where the air returns to room
23 temperature.

24 The longitudinal distance where each region begins and ends is approximately the same for
25 each of the set-point temperatures (Figure S3a). Similarly, the effect of flow rate on the
26 longitudinal temperature profile has been tested from 0.2 lpm to 1.0 lpm (Figure S3b) and the
27 position and length of each region is approximately the same for each flowrate. Since the length
28 of each region is independent of temperature and flow rate, the TD is characterized as follows:
29 the warming region is 15 cm, the heated region is 47 cm and the cooling region is 23 cm, which
30 includes some of the denuder section.

1 TD Model Inputs

2 As described previously, the TD consists of an active heating stage and a denuding stage.
3 Within the model, as the airstream moves through the TD it passes through five user defined
4 regions: the warming region (region A), the heated region (region B), the cooling region 1
5 (region C), the cooling region 2 (region D) and the cooled denuder (region E) (Figure S4). The
6 cooling region has been divided into two distinct regions because cooling occurs both within the
7 heating tube and the charcoal-denuder. The inner diameter of each region is different and since
8 gas-phase compounds are adsorbed by the activated charcoal in the denuder wall-losses are
9 treated differently in these two regions. The four regions are illustrated in Figure S4. All regions
10 are assumed to have a uniform temperature across the cross-sectional area of the tube.

11 The kinetic model of evaporation incorporates the TD geometry, flow characteristics, and
12 aerosol distribution parameters into the calculations. The tube diameter in regions A-C is 1.1 cm
13 and in region D and E is 0.95 cm.

15 Data Fitting: Best fit parameters

16 The best-fit parameters VFR_{max} , S_{VFR} and T_{50} determined by fitting Eq. 3 in the main text to
17 each of the experiments are given in Table S1. The VFR_{max} is the fit parameter that describes the
18 VFR at the maximum temperature and the VFR_{min} is the VFR at the low temperature limit. The
19 significance of S_{VFR} and T_{50} are discussed in the main text. VFR_{max} was held constant at zero for
20 all fits. The VFR_{max} at 298K from the model fit is constrained to be unity for each experiment to
21 be consistent with the observations.

23 Dimer Decomposition Model: Best fit parameters

24 In order to find the best fit model to the experimental observations for the dimer
25 decomposition kinetic model of evaporation in a thermodenuder, K_{eqm} was held constant while k_r
26 and ΔE_a were allowed to vary. It was found that good model-observation agreement could be
27 obtained over the range of K_{eqm} from 10^{-14} to 10^{-18} cm^3 molecules $^{-1}$. The corresponding k_r and
28 ΔE_a for each K_{eqm} are given in Table S2 along with the corresponding k_f . The Pearson's Chi-
29 squared value is given for each set of best-fit parameters. The best-fit model for $K_{eqm} = 10^{-16}$ and
30 10^{-17} have the lowest Chi-squared values. When these values were used to predict evaporation as
31 induced by isothermal dilution, the best-fit model for $K_{eqm} = 10^{-16}$ qualitatively agrees best with

1 observations (Vaden et al., 2011; Wilson et al., 2015); as such this was the best-fit model used as
2 the base case to explore the effects of the dilution factor, k_{loss} term and particle diameter (d_p) on
3 isothermal evaporation (Fig. 7).

4
5

6 **References**

7 Huffman, J. A., Ziemann, P. J., Jayne, J. T., Worsnop, D. R., and Jimenez, J. L.: Development
8 and characterization of a fast-stepping/scanning thermodenuder for chemically-resolved
9 aerosol volatility measurements, *Aerosol Science and Technology*, 42, 395-407,
10 10.1080/02786820802104981, 2008.

11 Vaden, T. D., Imre, D., Beránek, J., Shrivastava, M., and Zelenyuk, A.: Evaporation kinetics and
12 phase of laboratory and ambient secondary organic aerosol, *Proceedings of the National
13 Academy of Sciences of the United States of America*, 108, 2190-2195,
14 10.1073/pnas.1013391108, 2011.

15 Wilson, J., Imre, D., Beranek, J., Shrivastava, M., and Zelenyuk, A.: Evaporation Kinetics of
16 Laboratory-Generated Secondary Organic Aerosols at Elevated Relative Humidity,
17 *Environmental Science & Technology*, 49, 243-249, 2015.

18
19

1 **Table S1.** Fit parameters for all experimental mass thermograms.

Experiment Date	Initial C _{OA} (μg m ⁻³)	C _{OA} after dilution (μg m ⁻³)	VFR _{min}	S _{VFR}	T ₅₀ (K)
090512	1	n/a	1.09±0.01	-17.5±0.4	341±2
082912	9	n/a	1.12±0.07	-14.8±1.6	343±4
101912	30	n/a	1.07±0.03	-17.4±1.0	344±2
041114	90	n/a	1.08±0.02	-16.7±1.1	347±3
090712	150	n/a	1.11±0.03	-15.7±0.6	342±3
091312	180	n/a	1.08±0.01	-15.1±0.3	351±2
040914	200	n/a	1.08±0.02	-15.4±1.0	351±3
091212	400	n/a	1.04±0.01	-17.2±0.8	361±3
091112	600	n/a	1.06±0.01	-17.7±0.7	370±2
083112	600	n/a	1.09±0.03	-15.4±0.5	360±2
092412	650	n/a	1.04±0.01	-14.6±0.8	350±2
101812	800	n/a	1.02±0.00	-17.1±0.7	355±2
101212	380	5	1.11±0.02	-15.8±0.6	340±3
100912	380	6	1.09±0.02	-15.8±0.6	343±3
101112	430	7	1.10±0.02	-16.4±0.5	343±2
101712	500	7	1.12±0.03	-15.2±0.7	336±3
101612	450	8	1.00±0.02	-16.5±0.6	344±2
101012	450	10	1.15±0.03	-15.6±0.6	337±3
100412	450	24	1.12±0.03	-15.9±0.6	340±2

2

1

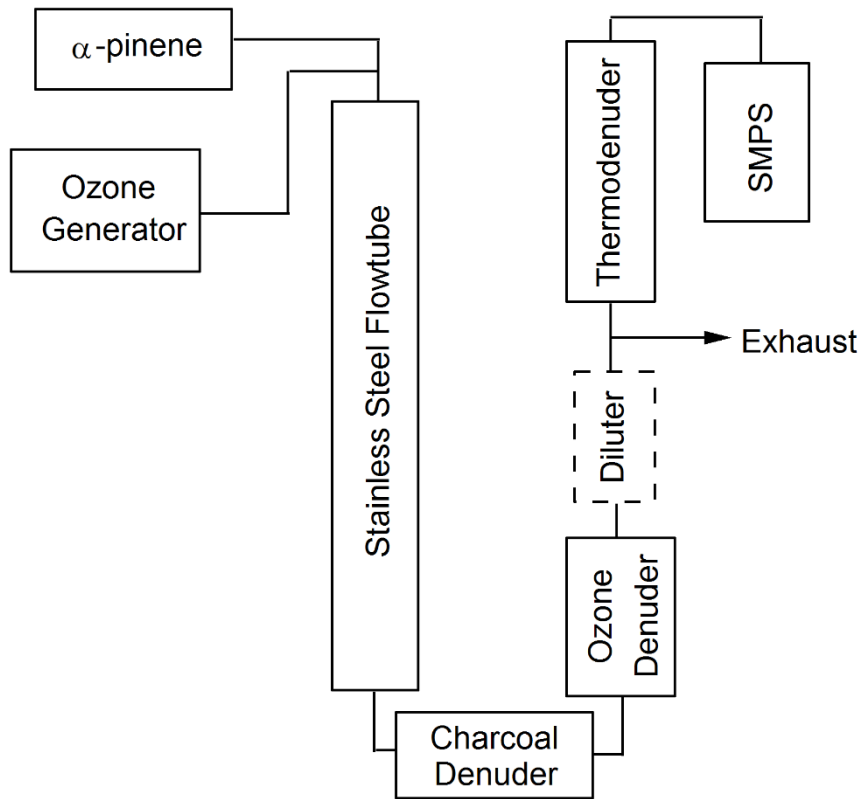
2 **Table S2.** The fit parameters from the best-fit dimer decomposition model for3 $K_{\text{eqm}} = 10^{-14}$ to 10^{-18} .

K_{eqm} ($\text{cm}^3 \text{ molecules}^{-1}$)	k_{r} (s^{-1})	ΔE_{a}	k_{f} ($\text{cm}^3 \text{ molecules}^{-1} \text{ s}^{-1}$)	χ^2
10^{-14}	0.0278	15.3	2.78×10^{-16}	0.2709
10^{-15}	0.0187	17.6	1.87×10^{-17}	0.2756
10^{-16}	0.00481	29.6	4.81×10^{-19}	0.1435
10^{-17}	0.00248	36.9	2.48×10^{-20}	0.1270
10^{-18}	0.00160	42.1	1.60×10^{-21}	0.2284

4

5

1

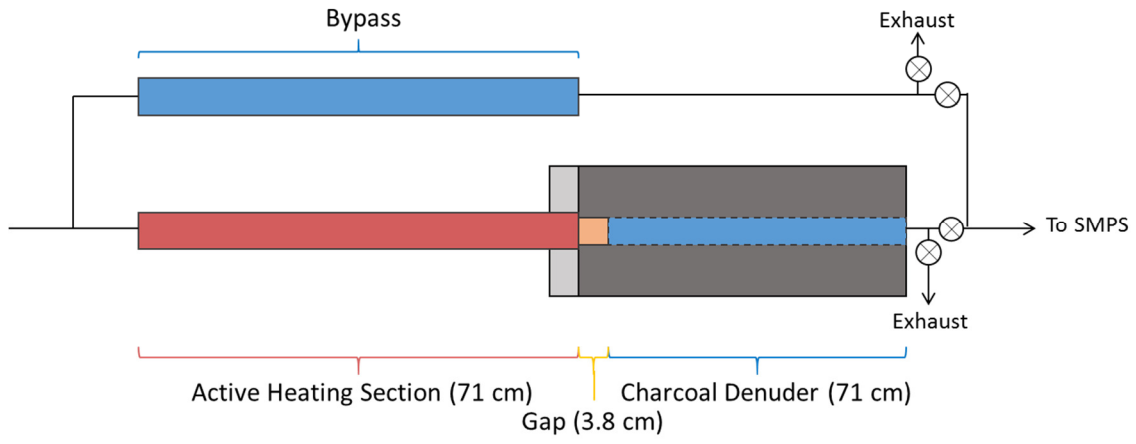


2

3 **Figure S1.** A schematic diagram of the experimental setup. Note that both the diluter and
4 thermodenuder contain bypass lines.

5

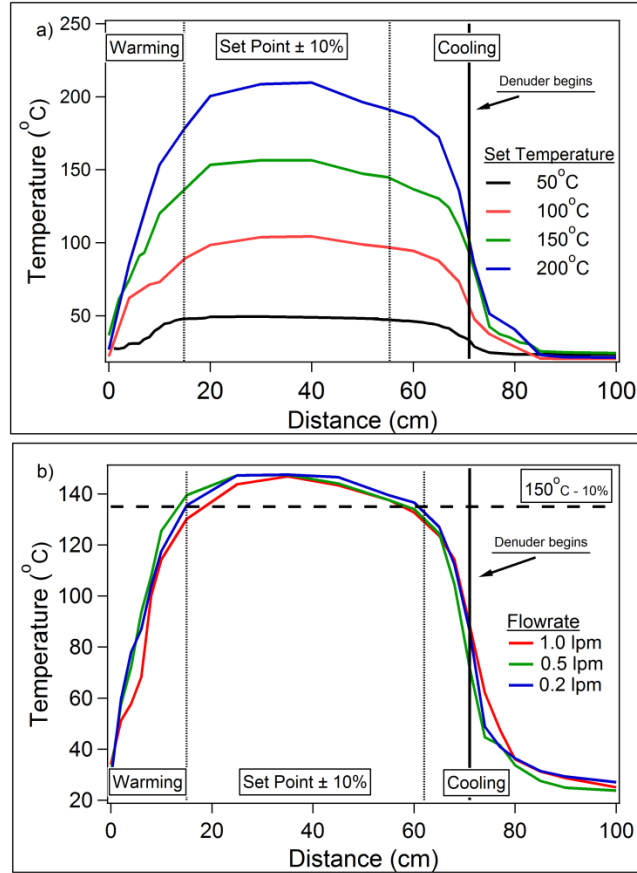
1



2

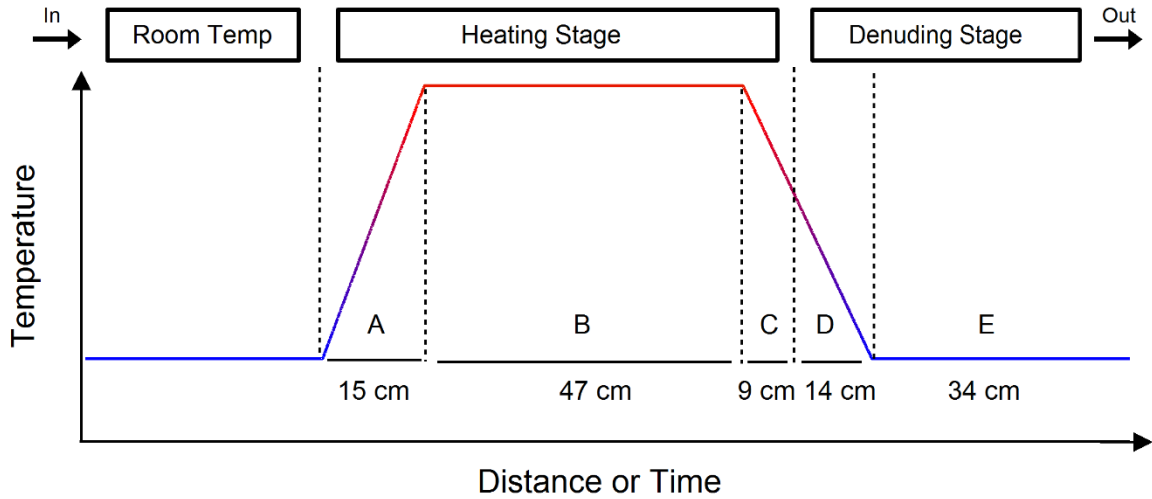
3 **Figure S2.** A schematic of the thermodenuder.

4



1
 2 **Figure S3.** (a) Longitudinal temperature profile of the TD measured for four set-point
 3 temperatures (50°C, 100°C, 150°C and 200°C). (b) Longitudinal temperature profile for three
 4 flow rates (1.0, 0.5 and 0.2 lpm) at a set-point temperature of 150 °C. The temperature profile is
 5 divided into three distinct sections (vertical gray lines): warming, heated (where the temperature
 6 is within 10% of the set point) and cooling. The thick, vertical black line at a distance of 71 cm
 7 indicates the beginning of the denuder.

8



1
 2 **Figure S4.** Schematic of the temperature profile used as inputs into the TD model. As the airflow
 3 enters the heated region there are three separate regions: the warming region 'A', the heated
 4 region 'B', and the cooling region 'C'. Note that the cooling region continues into the denuding
 5 stage (cooling region D). Region 'E' is the section of the denuding stage that is at room
 6 temperature.

7
 8